Solvent-Dependent Assembly of Terphenyl- and Quaterphenyldithiol on Gold and Gallium Arsenide

Dmitry A. Krapchetov,[†] Hong Ma,[‡] Alex K. Y. Jen,[‡] Daniel A. Fischer,[§] and Yueh-Lin Loo*,[†,||]

Chemical Engineering Department and Center for Nano- and Molecular Science and Technology, University of Texas at Austin, Austin, Texas 78712, Materials Science and Engineering Department, University of Washington, Seattle, Washington 98195, and Materials Science and Engineering Laboratory, National Institute of Standards and Technology, Gaithersburg, Maryland 20899

Received February 2, 2005. In Final Form: April 11, 2005

The assembly of terphenyldithiol (TPDT) and quaterphenyldithiol (QPDT) on gold and gallium arsenide from ethanol (EtOH), tetrahydrofuran (THF), and solutions consisting of both solvents has been characterized by near-edge X-ray absorption fine structure spectroscopy. The surface coverage and the average orientation of both TPDT and QPDT on gold are solvent-independent. These molecules readily form monolayers on gold with an ensemble-average backbone tilt of 30° ± 3° from the substrate normal. In sharp contrast, the assembly of TPDT and QPDT on gallium arsenide is extremely solvent-sensitive. At high ethanol fractions, both molecules form monolayers with an ensemble-average orientation that is indistinguishable from those on gold substrates. At low ethanol fractions and in pure THF, however, these molecules are disordered on gallium arsenide and the surface coverage is poor.

Introduction

The promise of nanoscale electronics[1]—in which individual molecules comprise the electrically active components—has instigated tremendous interest in molecular self-assembly. To date, a gamut of device assemblies have been demonstrated; these range from single-molecule nanojunctions[2−4] and nanopore devices[5,6] to soft-contact devices[7,8] where mercury, instead of a metallic solid, is used to electrically contact the organic molecules. While negative differential resistance,[9−13] rectification,[1,14,15] and other interesting electrical characteristics have been observed in devices that use complex organic molecules, such as rotaxanes,[16−18] many studies in this field remain focused on the nature of the electrical contact established between the metal electrode and the organic molecules.[19−21] As such, these studies have predominantly focused on simple straight-chain alkane systems that do not actually exhibit any interesting electrical behavior.

The organization of these molecules affects the way in which electrical contact is established between the metal electrode and the organic molecules. To this end, extensive structural characterization on alkylthiol self-assembled monolayers (SAMs) on coinage metal and semiconductor surfaces have been reported. These molecules, provided they are of sufficient length (generally more than 12 methylene units),[22−24] tend to spontaneously assemble on gold,[25−28] silver,[26,28,29] and gallium arsenide[24,26,30,31] surfaces

* Corresponding author: e-mail lloo@che.utexas.edu.
† Chemical Engineering Department, University of Texas at Austin.
‡ University of Washington.
§ National Institute of Standards and Technology.
|| Center for Nano- and Molecular Science and Technology, University of Texas at Austin.

(1) Aviram, A.; Ratner, M. A. *Chem. Phys. Lett.* **1974**, *29*, 277.
(2) Liang, W.; Shores, M. P.; Bockrath, M.; Long, J. R.; Park, H. *Nature* **2002**, *417*, 725.
(3) Reed, M. A.; Zhou, C.; Muller, C. J.; Burgin, T. P.; Tour, J. M. *Science* **1997**, *278*, 252.
(4) Zhitenev, N. B.; Meng, H.; Bao, Z. *Phys. Rev. Lett.* **2002**, *88*, 226801/1.
(5) James, D. K.; Tour, J. M. *Chem. Mater.* **2004**, *16*, 4423.
(6) Wang, W.; Lee, T.; Kretzschmar, I.; Reed, M. A. *Nano Lett.* **2004**, *4*, 643.
(7) Tran, E.; Rampi, M. A.; Whitesides, G. M. *Angew. Chem., Int. Ed.* **2004**, *43*, 3835.
(8) Selzer, Y.; Salomon, A.; Cahen, D. *J. Am. Chem. Soc.* **2002**, *124*, 2886.
(9) Tour, J. M.; Rawlett, A. M.; Kozaki, M.; Yao, Y.; Jagessar, R. C.; Dirk, S. M.; Price, D. W.; Reed, M. A.; Zhou, C. W.; Chen, J.; Wang, W.; Campbell, I. *Chemistry* **2001**, *7*, 5118.
(10) Salomon, A.; Arad-Yellin, R.; Shanzer, A.; Karton, A.; Cahen, D. *J. Am. Chem. Soc.* **2004**, *126*, 11648.
(11) Chen, J.; Reed, M. A.; Rawlett, A. M.; Tour, J. M. *Science* **1999**, *286*, 1550.
(12) Xue, Y.; Datta, S.; Hong, S.; Reifenberger, R.; Henderson, J. I.; Kubiak, C. P. *Phys. Rev. B* **1999**, *59*, R7852.
(13) Wassel, R. A.; Credo, G. M.; Fuierer, R. R.; Feldheim, D. L.; Gorman, C. B. *J. Am. Chem. Soc.* **2004**, *126*, 295.
(14) Metzger, R. M. *Chem. Rec.* **2004**, *4*, 291.
(15) Metzger, R. M. *Acc. Chem. Res.* **1999**, *32*, 950.
(16) Chen, Y.; Ohlberg, D. A. A.; Li, X.; Stewart, D. R.; Stanley, W. R.; Jeppesen, J. O.; Nielsen, K. A.; Stoddart, J. F.; Olynick, D. L.; Anderson, E. *Appl. Phys. Lett.* **2003**, *82*, 1610.
(17) Luo, Y.; Collier, C. P.; Jeppesen, J. O.; Nielsen, K. A.; Delonno, E.; Ho, G.; Perkins, J.; Tseng, H.-R.; Yamamoto, T.; Stoddart, J. F.; Heath, J. R. *ChemPhysChem* **2002**, *3*, 519.
(18) Heath, J. R. *Pure Appl. Chem.* **2000**, *72*, 11.
(19) Hsu, J. W. P.; Loo, Y. L.; Lang, D. V.; Rogers, J. A. *J. Vac. Sci. Technol., B* **2003**, *21*, 1928.
(20) Cui, X. D.; Zarate, X.; Tomfohr, J.; Sankey, O. F.; Primak, A.; Moore, A. L.; Moore, T. A.; Gust, D.; Harris, G.; Lindsay, S. M. *Nanotechnology* **2002**, *13*, 5.
(21) Hipps, K. W. *Science* **2001**, *294*, 536.
(22) Dubois, L. H.; Nuzzo, R. G. *Annu. Rev. Phys. Chem.* **1992**, *43*, 437.
(23) Dubois, L. H.; Zegarski, B. R.; Nuzzo, R. G. *J. Chem. Phys.* **1993**, *98*, 678.
(24) Ye, S.; Li, G.; Noda, H.; Uosaki, K.; Osawa, M. *Surf. Sci.* **2003**, *529*, 163.
(25) Karpovich, D. S.; Blanchard, G. J. *Langmuir* **1994**, *10*, 3315.
(26) Ulman, A. *Chem. Rev.* **1996**, *96*, 1533.
(27) Fischer, D.; Marti, A.; Hahner, G. *J. Vac. Sci. Technol., A* **1997**, *15*, 2173.
(28) Laibinis, P. E.; Whitesides, G. M.; Allara, D. L.; Tao, Y. T.; Parikh, A. N.; Nuzzo, R. G. *J. Am. Chem. Soc.* **1991**, *113*, 7152.
(29) Kondoh, H.; Nambu, A.; Ehara, Y.; Matsui, F.; Yokoyama, T.; Ohta, T. *J. Phys. Chem. B* **2004**, *108*, 12946.
(30) Baum, T.; Ye, S.; Uosaki, K. *Langmuir* **1999**, *15*, 8577.
(31) Tiberio, R. C.; Craighead, H. G.; Lercel, M.; Lau, T.; Sheen, C. W.; Allara, D. L. *Appl. Phys. Lett.* **1993**, *62*, 476.

10.1021/la0503000 CCC: $30.25
Published on Web 05/17/2005

Scheme 1. Synthesis of Acetyl-Protected Terphenyldithiol (TPDT) and Quaterphenyldithiol (QPDT)

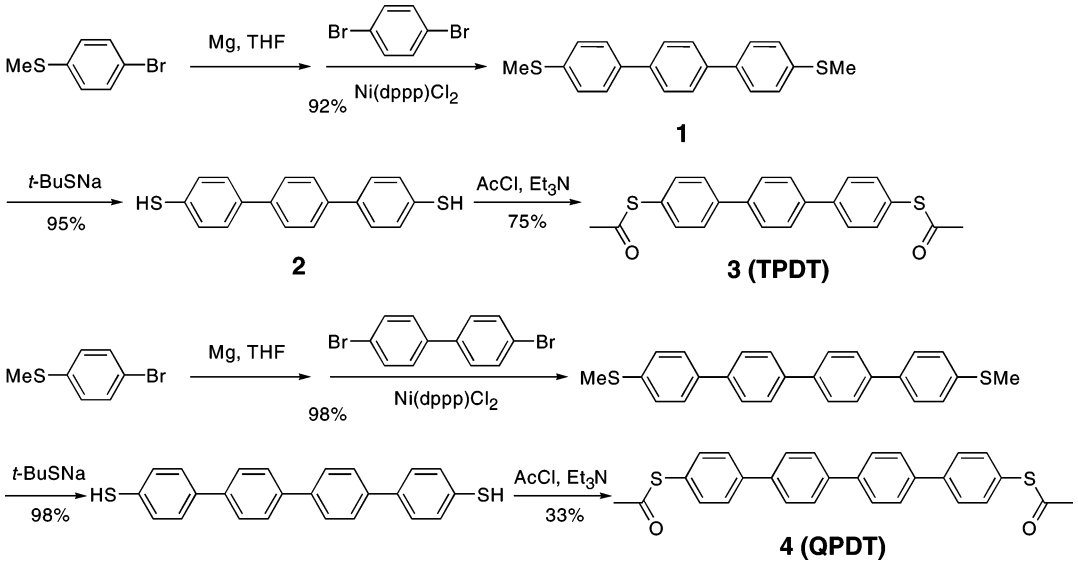

to form ordered monolayers. In contrast, the assembly of alkyldithiols—symmetric alkane molecules with thiol termination on both ends—appears to be more dependent on assembly conditions. For example, researchers recently showed by direct imaging that both 1,6-hexanedithiol[32] and 1,8-octanedithiol[33] generally lie flat on the substrate surface when assembled on gold and silver, respectively. Yet, in a series of papers that demonstrate additive contact pattering, Loo and co-workers[34−37] deduced that 1,8-octanedithiol must be bound to gallium arsenide on only one end in order to facilitate nanotransfer printing. Such an orientation was also previously reported by Rieley et al.[38] through a series of X-ray photoelectron spectroscopic experiments.

Compared to aliphatic systems, molecules containing simple aromaticity have backbone rigidity and ability to transport charge that are more akin to the electronically complex molecules of interest to the molecular electronics community. These molecules have therefore been identified as model systems for electrical studies. Recent reports, however, suggest that the assembly of these materials—critical to the fabrication of a functional device—is yet more complex than those of simple alkane systems.[39−44] In particular, the final structures of these assemblies are purportedly dependent on the details of processing conditions, including the types of substrates and solvents used. In light of this, we have chosen to elucidate the solvent effects of *n*-phenyldithiol (where $n = 3$ and 4) assemblies on gold and gallium arsenide substrates. Specifically, we have investigated the assembly of these molecules from ethanol (EtOH), tetrahydrofuran (THF), and solutions containing both solvents. This solvent pair was chosen because of an apparent solubility conflict: while EtOH is the most common solvent for assembling alkylthiol and conjugated monothiol molecules,[43−45] the longer *n*-phenyldithiols ($n = 3, 4$), in their thioacetyl forms (compounds **3** and **4** in Scheme 1), are poorly soluble in EtOH. These molecules, however, are completely soluble in THF. But THF is a poor solvent for the deprotecting agent, ammonium hydroxide (NH_4OH). Synchrotron-based near-edge X-ray absorption fine structure spectroscopy (NEXAFS) experiments suggest extreme solvent sensitivity when the molecules are assembled on freshly etched gallium arsenide. On the other hand, when the assembly is carried out on freshly deposited gold substrates, the process is solvent-independent.

Experimental Section

Synthesis of Dithiols. All the chemicals were purchased from Aldrich and used as received unless otherwise specified. THF used during the synthesis was distilled under nitrogen from sodium with benzophenone as the indicator. Methylene chloride was distilled over P_2O_5. ^{1}H NMR spectra (200 MHz) were taken on a Bruker-200 FT NMR spectrometer. ESI-MS spectra were obtained on a Bruker Daltonics Esquire ion trap mass spectrometer.

Compound 1. A Grignard solution was prepared via dropwise addition of a solution of 1-bromo-4-methylthiobenzene (10.56 g, 52.0 mmol) in dry THF (20 mL) to magnesium (1.33 g, 54.6 mmol) in dry THF (40 mL) under nitrogen. The combined solution was refluxed for 3.5 h. The resulting Grignard solution was cooled to room temperature and transferred to a suspension of 1,4-dibromobenzene (4.72 g, 20.0 mmol) and $Ni(dppp)Cl_2$ (0.11 g, 0.2 mmol) in dry THF (100 mL) at 0 °C under nitrogen. The mixture was stirred for 24 h under reflux, cooled, and poured into 1 N HCl solution (200 mL). The precipitate was filtered, washed with water, hexane, and methylene chloride, and dried overnight at 40 °C under vacuum to afford a light-yellow solid (5.90 g, 92%). ^{1}H NMR (200 MHz, $CDCl_3$) δ 7.65 (s, 4H), 7.55 (d, $J = 8.0$ Hz, 4H), 7.32 (d, $J = 8.0$ Hz, 4H), 2.55 (s, 6H). ESI-MS (*m/z*) calcd 322.1; found 322.0.

(32) Leung, T. Y. B.; Gerstenberg, M. C.; Lavrich, D. J.; Scoles, G.; Schreiber, F.; Poirier, G. E. *Langmuir* **2000**, *16*, 549.
(33) Cavallini, M.; Bracali, M.; Aloisi, G.; Guidelli, R. *Langmuir* **1999**, *15*, 3003.
(34) Loo, Y.-L.; Lang, D. V.; Rogers, J. A.; Hsu, J. W. P. *Nano Lett.* **2003**, *3*, 913.
(35) Loo, Y.-L.; Hsu, J. W. P.; Willett, R. L.; Baldwin, K. W.; West, K. W.; Rogers, J. A. *J. Vac. Sci. Technol., B* **2002**, *20*, 2853.
(36) Loo, Y.-L.; Willett, R. L.; Baldwin, K. W.; Rogers, J. A. *J. Am. Chem. Soc.* **2002**, *124*, 7654.
(37) Felmet, K.; Loo, Y.-L.; Sun, Y. *Appl. Phys. Lett.* **2004**, *85*, 3316.
(38) Rieley, H.; Kendall, G. K.; Zemicael, F. W.; Smith, T. L.; Yang, S. *Langmuir* **1998**, *14*, 5147.
(39) Azzam, W.; Wehner, B. I.; Fischer, R. A.; Terfort, A.; Woell, C. *Langmuir* **2002**, *18*, 7766.
(40) de Boer, B.; Meng, H.; Perepichka, D. F.; Zheng, J.; Frank, M. M.; Chabal, Y. J.; Bao, Z. *Langmuir* **2003**, *19*, 4272.
(41) Tai, Y.; Shaporenko, A.; Rong, H. T.; Buck, M.; Eck, W.; Grunze, M.; Zharnikov, M. *J. Phys. Chem. B* **2004**, *108*, 16806.
(42) Weckenmann, U.; Mittler, S.; Naumann, K.; Fischer, R. A. *Langmuir* **2002**, *18*, 5479.
(43) Frey, S.; Stadler, V.; Heister, K.; Eck, W.; Zharnikov, M.; Grunze, M.; Zeysing, B.; Terfort, A. *Langmuir* **2001**, *17*, 2408.
(44) Shaporenko, A.; Adlkofer, K.; Johansson, L. S. O.; Tanaka, M.; Zharnikov, M. *Langmuir* **2003**, *19*, 4992.
(45) Fuxen, C.; Azzam, W.; Arnold, R.; Witte, G.; Terfort, A.; Woell, C. *Langmuir* **2001**, *17*, 3689.

Dithiol 2. To a solution of **1** (Scheme 1) (1.00 g, 3.1 mmol) in anhydrous dimethylformamide (DMF, 25 mL) was added sodium *tert*-butylthiolate (1.04 g, 9.3 mmol). The reaction mixture was vigorously stirred and refluxed for 6 h under nitrogen.[46,47] The solution was cooled to room temperature and poured into 10% HCl solution (65 mL). The resulting precipitate was filtered off, washed with water and cold ethanol, and dried overnight at 40 °C under vacuum to afford a pale white solid (0.86 g, 95%). ^{1}H NMR (200 MHz, $CDCl_3$) δ 7.62 (s, 4H), 7.51 (d, $J = 8.2$ Hz, 4H), 7.36 (d, $J = 8.2$ Hz, 4H), 3.51 (s, 2H). ESI-MS (*m/z*) calcd 294.1; found 294.0.

TPDT 3. Due to the tendency for dithiol **2** to oxidize,[48] the thiol end groups were converted to thiolacetyl end groups. The thioacetyl end groups were then reconverted back to thiols during SAMs formation. To convert the thiols into thioacetyl groups, triethylamine (0.30 g, 3.0 mmol) followed by acetyl chloride (0.24 g, 3.0 mmol)[40,49] was added dropwise to a solution of dithiol **2** (Scheme 1) (0.40 g, 1.4 mmol) in dry methylene chloride (20 mL) under nitrogen. The mixture was stirred for 24 h at room temperature, poured into water, and extracted with methylene chloride. The combined methylene chloride layers were washed with water, dried with Na_2SO_4, and concentrated. The crude product was purified over silica gel column chromatography with hexane/methylene chloride (1:1) to methylene chloride as the eluents to afford a light-yellow solid (0.39 g, 75%). ^{1}H NMR (200 MHz, $CDCl_3$) δ 7.65−7.75 (m, 8H), 7.50 (d, $J = 7.8$ Hz, 4H), 2.46 (s, 6H). ESI-MS (*m/z*) calcd 378.1; found 378.1.

QPDT 4. This compound was synthesized with 4,4′-dibromobiphenyl as the starting material and by the same three-step procedure as that used for synthesizing compound TPDT **3** (Scheme 1). A slightly yellow solid was obtained. ^{1}H NMR (200 MHz, $CDCl_3$) δ 7.65−7.75 (m, 12H), 7.51 (d, $J = 8.0$ Hz, 4H), 2.47 (s, 6H). ESI-MS (*m/z*) calcd 454.1; found 454.0.

SAMs Formation. SureSeal grade solvents from Aldrich were used as received for SAMs formation. Polycrystalline gold substrates were prepared by evaporating 5 nm of Ti followed by 25 nm of Au onto polished silicon wafers (Wacker) in an evaporation chamber with a base pressure of $\approx 1 \times 10^{-7}$ Torr. These substrates were immediately transferred into a glovebox (MBraun, <0.1 ppm O_2, <0.1 ppm H_2O) for immersion in the assembly solutions. To remove the native oxide layer from GaAs, we etched single-side polished wafers [AXT, Si-doped, (100)] in concentrated HCl for 1 min, followed by rinsing with DI water and drying with a nitrogen stream. The GaAs substrates were immediately transferred into the glovebox and immersed in the dithiol solutions for molecular assembly.

Dithiol solutions were prepared by dissolving acetyl-protected terphenyldithiol (TPDT **3**) or quaterphenyldithiol (QPDT **4**) at 50 μM in either EtOH, THF, or solutions of EtOH and THF. Ammonium hydroxide at 25 μL/5 mL of solution was then added to facilitate an acid/base reaction with the thioacetyl end groups, resulting in thiol end groups.[48] After the addition of NH_4OH, the solutions were agitated for 1 min and left for an hour before freshly evaporated gold or freshly etched GaAs substrates were immersed into the solutions. The substrates remained immersed for 24 h before they were removed and were copiously rinsed with EtOH and dried in a stream of nitrogen. Due to the low solubility of acetyl-protected QPDT (**4** in Sheme 1) in EtOH, we were not able to assemble QPDT from pure EtOH. The complete range of EtOH/THF solution compositions was explored for TPDT.

NEXAFS. Near-edge X-ray absorption fine structure (NEXAFS) experiments were carried out at the NIST/Dow soft X-ray materials characterization facility located at beamline U7A at the National Synchrotron Light Source at Brookhaven National Laboratories.[50] The partial electron yield (PEY) NEXAFS spectra were acquired at the carbon K-edge with a retarding entrance grid bias of −150 V for enhanced surface sensitivity.[51] Polarized synchrotron soft X-rays with a polarization factor, P, of ≈85% were used.[52] We used a scan step of 0.1 eV in the region of interest (280−310 eV) and a 0.2 eV scan step at the pre- and post-edge regions. The spectra were collected in a vacuum ($\approx 1 \times 10^{-8}$ Torr) at ambient temperature. To evaluate monolayer coverage, polarization-independent sample spectra were acquired at an X-ray incident angle (defined as the angle between the incidence beam and the substrate plane) of 55°, also known as the magic angle.[53] Angle-dependent NEXAFS data were obtained by varying the X-ray incident angle between 20° (grazing) and 75° (near-normal). Compilation of angle-dependent data allowed us to estimate the ensemble-average orientation of the molecules with respect to the surface.[54,55]

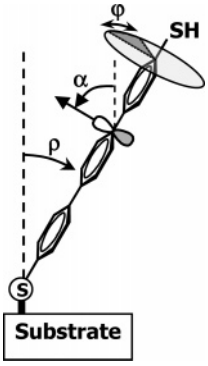

Figure 1. Schematic of a TPDT molecule adsorbed on a substrate. The angles used in our analysis are identified.

Raw PEY NEXAFS spectra were normalized by the corresponding incident beam intensity, I_0, obtained concomitantly from the photo yield of a freshly coated gold grid that is located upstream from the sample chamber. This normalization accounts for any incident beam intensity fluctuations and monochromator absorption features.[56] We corrected the background curvature of assemblies on gold by dividing each sample spectrum by that of bare gold.[53] Sample spectra obtained on gallium arsenide substrates were normalized by I_0 but not background-corrected. Quantitative analyses of angle-dependent NEXAFS data were carried out after the removal of an isotropic background that was generated from comparison of the difference spectra.[55,57]

The angle-dependent NEXAFS data were analyzed according to the building block (BB) model[57,58] to obtain the ensemble-average molecular orientation of the assemblies. We chose the π^* resonance at 285 eV—the most intense spectral feature—for quantitative analysis of the molecular orientation. The π^* resonance intensity, I_v, that originates from the corresponding vector orbital, if 3-fold substrate symmetry is assumed, can be described by[53,55]

$$I_v(\alpha, \theta) = A\{{}^1/_3P[1 + {}^1/_2(3\cos^2\theta - 1)(3\cos^2\alpha - 1)] + {}^1/_2(1 - P)\sin^2\alpha\} \quad (1)$$

where A is a proportionality constant, P is the X-ray polarization factor (≈85% in our setup), θ is the X-ray incident angle, and α is the angle between the orbital vector and the substrate normal. Figure 1 contains a scheme of an adsorbed molecule, and it

(46) Pinchart, A.; Dallaire, C.; Van Bierbeek, A.; Gingras, M. *Tetrahedron Lett.* **1999**, *40*, 5479.
(47) Kang, J. F.; Ulman, A.; Liao, S.; Jordan, R.; Yang, G.; Liu, G.-Y. *Langmuir* **2001**, *17*, 95.
(48) Tour, J. M.; Jones, L.; Pearson, D. L.; Lamba, J. J. S.; Burgin, T. P.; Whitesides, G. M.; Allara, D. L.; Parikh, A. N.; Atre, S. *J. Am. Chem. Soc.* **1995**, *117*, 9529.
(49) Pearson, D. L.; Tour, J. M. *J. Org. Chem.* **1997**, *62*, 1376.
(50) For detailed information on the NIST/Dow Soft X-ray Materials Characterization Facility at NSLS BNL, see http://www.nsls.bnl.gov/newsroom/publications/newsletters/1996/96-nov.pdf.
(51) Genzer, J.; Kramer, E. J.; Fischer, D. A. *J. Appl. Phys.* **2002**, *92*, 7070.
(52) Genzer, J.; Sivaniah, E.; Kramer, E. J.; Wang, J.; Koerner, H.; Char, K.; Ober, C. K.; DeKoven, B. M.; Bubeck, R. A.; Fischer, D. A.; Sambasivan, S. *Langmuir* **2000**, *16*, 1993.
(53) Stohr, J. *NEXAFS Spectroscopy*; Springer: Berlin, 1992.
(54) Outka, D. A.; Stohr, J.; Rabe, J. P.; Swalen, J. D.; Rotermund, H. H. *Phys. Rev. Lett.* **1987**, *59*, 1321.
(55) Stohr, J.; Outka, D. A. *Phys. Rev. B* **1987**, *36*, 7891.
(56) Fischer, D. A.; Efimenko, K.; Bhat, R. R.; Sambasivan, S.; Genzer, J. *Macromol. Rapid Commun.* **2004**, *25*, 141.
(57) Kinzler, M.; Schertel, A.; Haehner, G.; Woell, C.; Grunze, M.; Albrecht, H.; Holzhueter, G.; Gerber, T. *J. Chem. Phys.* **1994**, *100*, 7722.
(58) Outka, D. A.; Stoehr, J.; Rabe, J. P.; Swalen, J. D. *J. Chem. Phys.* **1988**, *88*, 4076.

illustrates the different angles that are involved in this analysis. From a geometrical standpoint:

$$\cos^2 \alpha = \cos^2 \phi \sin^2 \rho \quad (2)$$

Equation 2 can be equivalently expressed as

$$\sin^2 \alpha = 1 - \cos^2 \phi \sin^2 \rho \quad (3)$$

where ρ is the tilt angle of the molecular axis away from the substrate normal (see Figure 1) and ϕ is the ring-plane twist angle, which is defined as the angle between the π transition dipole moment vector of the phenyl rings and the plane spanned by the molecular axis and the substrate normal. The average molecular tilts were estimated on the basis of previously published procedures[55,57] where the π^* integrated resonance intensity as a function of X-ray incident angle is fitted to eq 1. During this exercise, A and ρ are floating parameters. We assumed a planar backbone (i.e., successive phenyl rings are coplanar) and a twist angle, $\phi = 32°$,[43,44,59] on the basis of experimental findings for oligo(phenylene-ethynylene)thiols[60,61] and theoretical studies of biphenylthiols.[62]

Ellipsometry. The thickness of the molecular assemblies on gold was measured with a spectroscopic ellipsometer (J. A. Woollam Co.). Measurements were carried out between 220 and 500 nm; the data were collected at incidence angles of 60°, 65°, and 70° with respect to the substrate normal. Optical constants for bare gold substrates were obtained from the same batches of freshly evaporated gold on which SAMs were formed. We were, however, unable to obtain reproducible optical constants for bare gallium arsenide because these substrates tend to oxidize when exposed to ambient conditions.[63,64] A refractive index of 1.55[40] for TPDT and QPDT was assumed during the analysis. We measured average thicknesses of 17 ± 1 Å and 23 ± 2 Å for TPDT and QPDT on gold, respectively, for the entire range of solvent composition examined. These values are similar to those reported for the corresponding monothiols[65] and are generally in accord with the theoretical molecular lengths of 17.6 and 22.1 Å for TPDT and QPDT, respectively.[40] We deduced from these measurements that TPDT and QPDT form monolayers on gold, and the molecules are generally oriented upright. This is further supported by quantitative NEXAFS analysis below. Our NEXAFS analysis will also show that TPDT and QPDT form comparable assemblies on gallium arsenide at high ethanol volume fractions, hereafter referred to as EFs, in the assembly solution. We therefore believe TPDT and QPDT to also form monolayers on gallium arsenide. We are presently developing protocols to reproducibly measure the thicknesses of SAMs on gallium arsenide.

Results and Discussion

Figure 2 contains polarization-independent, pre-edge normalized NEXAFS spectra of TPDT and QPDT assemblies on gold (Figure 2a,b) and gallium arsenide (Figure 2c,d), respectively. The spectral features are identified in Figure 2a: we observe a resonance at 285 eV (π^*) attributed to the C1s $\rightarrow \pi^*_{C=C}$ transition[55] in TPDT and QPDT, and we can also identify broad resonances at 293 and 303 eV originating from the C1s $\rightarrow \sigma_1^*$ and σ_2^* transitions,[55] respectively. Additionally, we observe spectral features at 287.4 and 288.8 eV; these resonances have previously been assigned to the R*/C−S* and π_2^* transitions.[55] Finally, we observe a peak at 290.2 eV; this peak

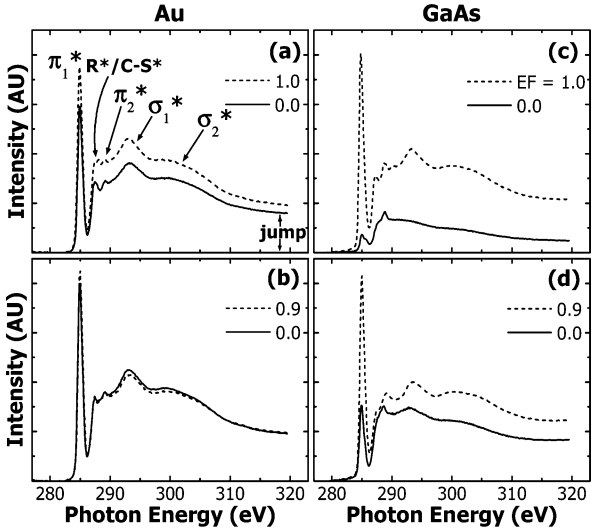

Figure 2. C 1s polarization-independent, pre-edge normalized PEY NEXAFS spectra of (a) TPDT on gold, (b) QPDT on gold, (c) TPDT on gallium arsenide, and (d) QPDT on gallium arsenide acquired at the magic angle (55°). The molecules were assembled from either pure EtOH (a and c, ---), a solution at ethanol fraction = 0.9 (b and d, ---), or from pure THF (—). Relevant absorption resonances are identified in panel a.

is more prominent in the spectra acquired on gallium arsenide samples assembled at low ethanol volume fractions (EFs). We are presently uncertain about its peak assignment; its presence does not affect the conclusions drawn in this discussion as it is not used in our quantitative analysis. We speculate, however, that this peak is associated with the C1s $\rightarrow \pi^*_{C=O}$ transition originating from incomplete deprotection of the thioacetyl end groups of the molecules (see chemical structures **3** and **4** in Scheme 1).[66] This hypothesis is consistent with our preliminary Fourier transform infrared spectroscopy experiments where a C=O carbonyl stretching mode (1706 cm^{-1})[40] is observed in our SAMs despite the addition of NH_4OH (which facilitates the conversion of thioacetyl to thiol end groups) during assembly;[67] this signal diminishes upon further exposure of the SAMs to NH_4OH.

Differences in the polarization-independent, pre-edge normalized NEXAFS spectra of TPDT and QPDT reflect real differences in the SAMs structure. The dashed lines in Figure 2 represent the NEXAFS spectra of molecules assembled from an EtOH-rich solution, while the solid lines represent the NEXAFS spectra of molecules assembled from a THF solution. The NEXAFS spectra acquired on both TPDT and QPDT on gold are largely identical (Figure 2a,b). This observation suggests that varying EF does not have an adverse effect on the quality of the SAMs on gold. On the other hand, Figure 2 panels c and d reveal drastically different NEXAFS spectra for samples assembled from the two different solvents on gallium arsenide, indicating that assemblies on gallium arsenide are extremely sensitive to the types of solvent. Specifically, we see a sharp decrease in both the π^* resonance intensity and the overall PEY signal in the samples assembled from THF, suggesting a different structure within and coverage of the SAMs.

To elucidate the structural differences in these SAMs, we examined the NEXAFS spectra to quantify the molecular coverage as well as the ensemble-average molecular orientation. The NEXAFS spectra shown in

(59) Dzyabchenko, A.; Scheraga, H. A. *Acta Crystallogr.* **2004**, *B60*, 228.
(60) Stapleton, J. J.; Harder, P.; Daniel, T. A.; Reinard, M. D.; Yao, Y.; Price, D. W.; Tour, J. M.; Allara, D. L. *Langmuir* **2003**, *19*, 8245.
(61) Dhirani, A.-A.; Zehner, R. W.; Hsung, R. P.; Guyot-Sionnest, P.; Sita, L. R. *J. Am. Chem. Soc.* **1996**, *118*, 3319.
(62) Chang, S.-C.; Chao, I.; Tao, Y.-T. *J. Am. Chem. Soc.* **1994**, *116*, 6792.
(63) Torkhov, N. A. *Semiconductors* **2003**, *37*, 1177.
(64) Moriarty, P.; Hughes, G. *Ultramicroscopy* **1992**, *42−44*, 956.
(65) Himmel, H.-J.; Terfort, A.; Woell, C. *J. Am. Chem. Soc.* **1998**, *120*, 12069.
(66) Urquhart, S. G.; Ade, H. *J. Phys. Chem. B* **2002**, *106*, 8531.
(67) Krapchetov, D.; Loo, Y.-L. Unpublished results, 2005.

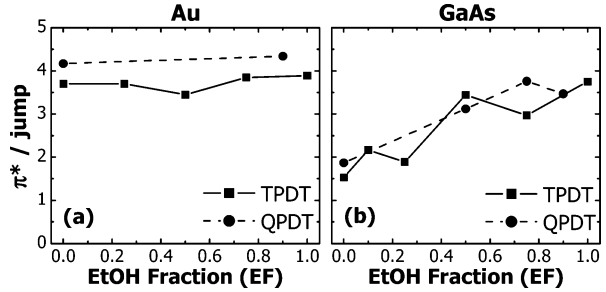

Figure 3. NEXAFS π^*/jump ratios for TPDT and QPDT on (a) gold and (b) gallium arsenide as a function of EF in the assembly solution. π^*/jump reflects the monolayer coverage on the surface. At high EFs, the monolayer coverage on gallium arsenide approaches that on gold.

Figure 2 were acquired at the magic angle (55°); data at this angle are independent of p- and s-state transitions of the X-ray source.[53] As such, the spectra shown in Figure 2 are independent of the details of the molecular orientation and can be directly compared with one another. To quantify the molecular coverage in these SAMs, we plot the ratio of the integrated intensity of the π^* resonance at 285 eV and the magnitude of the carbon-edge jump in Figure 3. Since the π^* integrated intensity solely emanates from the phenyl rings in the molecules and the magnitude of the edge jump is a reflection of the total carbon content on the surface, this ratio discounts the presence of carbon contaminants, if any, on the surface, thereby accurately reflecting the molecular coverage in our samples. We shall refer to this ratio as π^*/jump throughout our discussion.

We have quantified π^*/jump as a function of EF for assemblies on gold and gallium arsenide in Figure 3, panels a and b, respectively. On gold, π^*/jump is constant over the entire range of EF examined for both TPDT and QPDT. Such data indicate a solvent-independent surface coverage for both molecules on gold. In contrast, we observe that π^*/jump increases with increasing EF for assemblies on gallium arsenide, implying progressively increasing coverage with increasing EtOH content in the assembly solution. Furthermore, the π^*/jump for gallium arsenide assemblies at high EF approach those extracted from gold assemblies, suggesting comparable monolayer coverage for both TPDT and QPDT on gold and gallium arsenide at high EFs.

Quantitative analysis of the pre- and post-edge normalized NEXAFS spectra acquired at varying X-ray incident angles—shown for TPDT on gold in Figure 4a,b—completes the picture. We observe that the resonance intensities in these spectra vary with the X-ray incident angle: the π^* resonance grows while the σ^* resonances diminish with increasing incident angle. This phenomenon, dichroism,[53] where the π^* resonance grows at the expense of the σ^* resonances, is a strong indication that the molecules are preferentially oriented. That TPDT is preferentially oriented on gold is further substantiated by the difference spectra shown in the lower portions of Figure 4a,b. The difference spectra are obtained by subtracting the NEXAFS spectra at 20° from the NEXAFS spectra at other incident angles, that is, $I(\theta) - I(20°)$. The difference spectra therefore emphasize the angle-dependent spectral features. The ensemble-average orientation of the SAMs can be qualitatively determined from the way in which the orbitals interact with the electric field of the incident X-rays. Specifically, our data indicate that the π^* orbitals of the molecules are oriented nearly parallel to the X-ray electric field vector, **E** (hence maximal intensity of the π^* resonance in this configuration), while

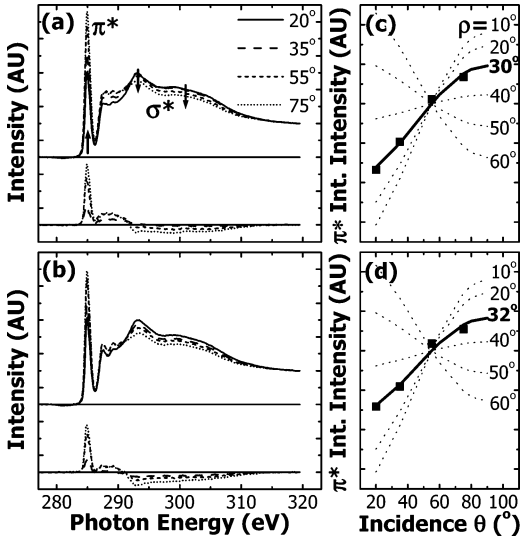

Figure 4. C 1s angle-dependent, pre- and post-edge normalized NEXAFS spectra of TPDT monolayers on gold assembled from (a) ethanol and (b) THF acquired at the indicated angles of X-ray incidence. The difference spectra (bottom portions of plots) emphasize angle-dependent resonances and are offset along the *y*-axis for clarity. The π^* integrated peak intensities as a function of incidence angle, and the corresponding theoretical fits to eq 1, are shown in panels c and d. The best fits (solid lines) and the resulting tilt angles are highlighted. The uncertainty of NEXAFS analysis is estimated to be ±3°.

the σ^* planes lie nearly perpendicular to **E** when the incident X-rays are at 75° from the substrate. Accordingly, at grazing incident X-rays, the π^* orbitals must be oriented nearly perpendicular (hence minimal intensity of the π^* resonance in this configuration), while the σ^* planes must lie nearly parallel to **E**. It follows that the molecules must be oriented generally upright in order to satisfy the dipole selection rules.[55]

We have quantified the ensemble-average molecular orientation by analyzing the angular dependence of the π^* resonance according to the BB model.[57,58] To extract the integrated intensity of each resonance, we fit the entire NEXAFS spectra to a series of Gaussian functions (the peak widths and peak locations were determined from the difference spectra) and a C1s → continuum transition edge. The extracted integrated π^* intensities for Figure 4 panels a and b as a function of incident angle, along with their theoretical fits to eq 1, are shown in Figure 4 panels c and d, respectively. In each case, the best fit, along with the resulting tilt angle, ρ, is highlighted. The dashed lines are graphical representations of eq 1 at other specified tilt angles. Our analysis indicates that TPDT assumes an ensemble-average tilt of ≈30° away from the substrate normal on gold substrates regardless of the assembly solvent. We note, from the fits (dashed and solid lines) shown in Figure 4c,d, that NEXAFS analysis does not distinguish between the following two scenarios: when the sample consists of disordered molecules and when the sample consists of oriented molecules with an ensemble-average tilt of 43° away from the substrate normal. In both these cases, the integrated π^* intensities are independent of the X-ray incident angle. This limitation results from the 3-fold substrate symmetry assumed during our analysis, where the orbital tilt, α, and the incident angle, θ, are mathematically equivalent in eq 1. There therefore exists a "magic orientation" at $\alpha = 55°$ where the NEXAFS intensities appear to be incident angle-independent. Since we assumed $\phi = 32°$ in our analysis,

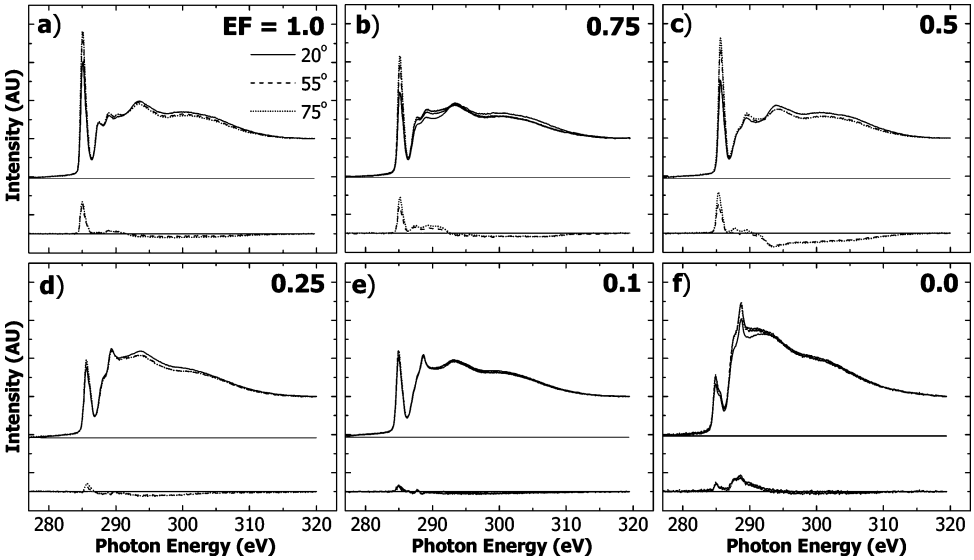

Figure 5. C 1s angle-dependent, pre- and post-edge normalized PEY NEXAFS spectra acquired at 20°, 55°, and 75° X-ray incidence of TPDT on gallium arsenide assembled at varying EFs. The difference spectra are offset along the *y*-axis for clarity.

Table 1. Ensemble-Average Molecular Tilt[a] of TPDT and QPDT Monolayers on Gold

	ethanol fraction (EF)					
	0	0.25	0.5	0.75	0.9	1
TPDT	32 ± 3	29 ± 3	26 ± 3	30 ± 3		30 ± 3
QPDT	28 ± 3				28 ± 3	

[a] Molecular tilt values are given in degrees.

Table 2. Ensemble-Average Molecular Tilt[a] of TPDT and QPDT Monolayers on Gallium Arsenide

	ethanol fraction (EF)					
	0	0.25	0.5	0.75	0.9	1
TPDT	DIS[b]	DIS	35 ± 3	35 ± 3		33 ± 3
QPDT	DIS		39 ± 3	24 ± 3	27 ± 3	

[a] Molecular tilt values are given in degrees. [b] DIS denotes monolayers that do not exhibit any preferential molecular orientation.

the magic orientation results when the ensemble-average molecular tilt happens to be 43°.

The assembly of QPDT on gold substrates is qualitatively similar to TPDT assembly. QPDT spontaneously adsorbs on gold to form ordered monolayers that are tilted on average ≈28° away from the substrate normal; this average orientation also appears to be independent of assembly solvent. The uncertainty of the calculated tilt angles is estimated to be ±3°, on the basis of experimental uncertainties and the uncertainty associated with the assumed twist angle and phenyl backbone planarity.[68−70] The tilt angles of both TPDT and QPDT assemblies on gold at varying EF are listed in Table 1. Our analysis indicates that both TPDT and QPDT readily form ordered monolayers on gold substrates; the extent of coverage and the ensemble-average molecular orientation appears to be independent of the assembly solvent. In fact, the tilt angles we obtain for TPDT are consistent with those reported for terphenylthiol (TPT) monolayers on gold,[43,45,65] suggesting that the addition of a functional group in the dithiol molecules does not impact the average molecular orientation appreciably.

NEXAFS experiments on TPDT and QPDT assembled on gallium arsenide substrates tell a dramatically different story. The incident angle-dependent pre- and post-edge normalized NEXAFS spectra of TPDT as a function of EF are shown in Figure 5. The corresponding difference spectra are also shown to illustrate changes in dichroism as a function of EF. Contrary to the SAMs on gold, the assembly of TPDT on gallium arsenide appears to be extremely sensitive to the amount of ethanol in the assembly solution. In Figure 5a−c, the π^* resonance grows at the expense of the σ^* resonances when the X-ray incident angle is increased. This trend—similar to that observed in TPDT and QPDT assemblies on gold—suggests that TPDT is preferentially oriented upright. In contrast, the samples assembled in EtOH-poor solvents exhibit little change in their respective angle-dependent NEXAFS spectra (Figure 5d−f). Their corresponding difference spectra also indicate near-zero intensity, suggesting disordered monolayers in these samples with the exception of Figure 5f. The nonzero difference spectrum in Figure 5f is attributed to small differences in the angle-dependent NEXAFS spectra; since the surface coverage of TPDT in this sample is poor, we attribute these small differences to (small amounts of) contaminants on the surface. Of the oriented samples, we are able to quantify the tilt angles using the procedures described previously; results are summarized in Table 2. At high EFs (>0.5), TPDT and QPDT form ordered monolayers; the extracted tilt angles are not dissimilar from those extracted from gold assemblies. The similarity in monolayer coverage and ensemble-average molecular orientation suggests that gold and gallium arsenide assemblies at high EF are structurally comparable. Decreasing EF, however, produces monolayers with progressively larger ensemble-average tilt angles on gallium arsenide; at small EFs (<0.25), the monolayers are completely disordered. This trend is also in accord with what we observe in terms of monolayer coverage.

That the assembly of TPDT and QPDT on gallium arsenide is solvent-dependent is not surprising. Indeed, solvent-dependent assembly has been previously reported for conjugated SAMs. For example, Ishida et al.[71] presented evidence for phase separation when terphenylthiol (only one thiol end group on the molecule) was assembled

(68) Corish, J.; Morton-Blake, D. A.; O'Donoghue, F.; Baudour, J. L.; Beniere, F.; Toudic, B. *THEOCHEM* **1995**, *358*, 29.
(69) Cailleau, H.; Baudour, J. L.; Zeyen, C. M. E. *Acta Crystallogr.* **1979**, *B35*, 426.
(70) Baudour, J. L.; Delugeard, Y.; Rivet, P. *Acta Crystallogr.* **1978**, *B34*, 625.

from methylene chloride on gold. When TPT was assembled from EtOH, however, ordered, densely packed SAMs were observed by scanning tunneling microscopy. Solvent effects on assembly were also previously reported in alkylthiol assemblies on nickel. Mekhalif et al.[72] reported the formation of high-quality SAMs when a polar solvent was used, whereas an apolar solvent yields little assembly. These reports were all based on assemblies on metal surfaces. What is surprising in our case is that such solvent dependence is observed only on gallium arsenide but not on gold. While the origin of this phenomenon remains uncertain, the observed disparity must arise from differences in solvent−molecule−substrate interactions in the two systems. In the case of gold assemblies, it is well-known that the tendency to form S−Au bonds is very strong,[22,26] so much so that thioacetyl-terminated molecules can spontaneously adsorb on gold substrates without prior deprotection.[48] Indeed, our own preliminary Fourier transform infrared experiments reveal that thioacetyl-terminated molecules can spontaneously adsorb on gold. The molecule−substrate interactions in such systems must therefore dominate the assembly process; they easily outweigh any possible solvent−molecule or solvent−substrate interactions. On the other hand, little is known about molecular assembly on semiconductor surfaces despite recent studies of alkylthiols[24,30] and conjugated thiols[44,73] on gallium arsenide. We speculate that the molecule−substrate interactions in gallium arsenide assemblies are weaker than those in gold. As such, the solvent quality plays a significant role, and the final structure of these assemblies depends on the details of solvent−molecule and solvent−substrate interactions.

Conclusions

We report the solvent effects of TPDT and QPDT assemblies on both gold and gallium arsenide substrates investigated by NEXAFS. Both molecules readily adsorb on gold substrates to form ordered SAMs with high monolayer coverage independent of assembly solvent. Quantitative analysis of angle-dependent NEXAFS spectra yields tilt angles of 30° and 28° from the substrate normal for TPDT and QPDT, respectively. In sharp contrast to gold assemblies, TPDT and QPDT adsorption on gallium arsenide is highly solvent-sensitive. The monolayer coverage increases monotonically with increasing ethanol fraction in the assembly solvent. Correspondingly, the molecules within the SAMs become upright. At high ethanol fractions and in pure ethanol, the monolayer coverage and the molecular orientation in gallium arsenide assemblies approach those observed in gold assemblies.

Acknowledgment. Funding from the NSF (DMR-0314707), the Camille and Henry Dreyfus Foundation, and the Keck Foundation to Y.L.L. is gratefully acknowledged. A.K.Y.J. acknowledges funding from the AFOSR-Bioinspired Concept and ARO-DURINT. Additionally, Y.L.L. and D.A.K. thank Professors Mike White, Jan Genzer, and Erin Jablonski, and Dr. Sharadha Sambasivan for useful discussions.

LA0503000

(71) Ishida, T.; Mizutani, W.; Azehara, H.; Sato, F.; Choi, N.; Akiba, U.; Fujihira, M.; Tokumoto, H. *Langmuir* **2001**, *17*, 7459.

(72) Mekhalif, Z.; Laffineur, F.; Couturier, N.; Delhalle, J. *Langmuir* **2003**, *19*, 637.

(73) Shaporenko, A.; Adlkofer, K.; Johansson, L. S. O.; Ulman, A.; Grunze, M.; Tanaka, M.; Zharnikov, M. *J. Phys. Chem. B* **2004**, *108*, 17964.